Sensors and Actuators A 149 (2009) 7–15

Contents lists available at ScienceDirect

Sensors and Actuators A: Physical

journal homepage: www.elsevier.com/locate/sna

# Measurement of dynamic lubricating oil film thickness between piston ring and liner in a motored engine

Atul Dhar[a], Avinash Kumar Agarwal[a,*], Vishal Saxena[b]

[a] Engine Research Laboratory, Department of Mechanical Engineering, Indian Institute of Technology Kanpur, Kanpur, 208016, India
[b] Department of Electrical Engineering, Indian Institute of Technology Kanpur, Kanpur 208016, India

ARTICLE INFO

*Article history:*
Received 15 August 2008
Received in revised form
12 September 2008
Accepted 28 September 2008
Available online 19 October 2008

*Keywords:*
Capacitance sensor
Piston ring
Minimum oil film thickness
Micro-sensors
Wear
Particulate

ABSTRACT

The interface between the piston rings and cylinder liner plays an important role in total frictional losses and mechanical wear of internal combustion engines and is increasingly coming under scrutiny as legislated particulate emission standards are becoming more and more stringent. The capacitance method is used for measurement of minimum oil film thickness at the piston ring–liner interface in the present investigations. Measurement of capacitance formed between the piston ring and a probe mounted flush with the liner provides an accurate measurement of oil film thickness provided that the region between the probe and liner is flooded with lubricating oil whose dielectric constant is known. This paper presents detailed design of sensor, instrumentation and measurement of lubricating oil film thickness using capacitive micro-sensor. The present investigation is carried out in a motored engine in order to validate the sensor and instrumentation and it can be directly employed in a firing engine also.

The oil film thickness was measured at different speeds at three different locations, i.e. close to TDC, mid stroke position and close to BDC position and the results are accordingly presented in this paper. Lubricating oil film thickness is found to vary between 0.2 and 8 μm in the motored engine. At a particular position, lubricating oil film thickness varies significantly in upward and downward stroke of the engine due to reversal in direction of piston tilt.



## 1. Introduction

Oil consumption is a major concern for all engines; however the causes are not clearly understood. In order to be able to design future engines to have low oil consumption levels, a more complete understanding of the mechanisms of oil consumption is required. The objective of this work was to utilize the capacitance probe technique to investigate oil transport and consumption in a motored diesel engine. Understanding the mechanism of lubrication between cylinder liner and piston ring is important for reducing the engine emissions as well as increasing the engine efficiency. Lubricating oil combustion contributes 2–25% (w/w) to the total particulate emission and 16–80% to the extractable organic fraction of the particulates and this can be significantly reduced by controlling the oil film thickness between the piston ring and the liner [1]. To understand transient oil transport, research in last two decades involved measurement of oil film thickness using various methods such as capacitance method, resistance method, inductance method, and optical methods [2–10]. The piston motion, ring profile, liner surface roughness and lubricating oil properties play a very important role in controlling the oil film thickness [11,12]. The oil film thickness is very critical even during lower engine loads since at lower loads, the film thickness is relatively higher and higher amount of lubricating oil gets thrown into the combustion chamber and thus lubricating oil contribution to the particulate formation becomes higher at lower loads. At high loads (near full load), the oil film thickness becomes critical because of very high cylinder pressures which may reach a critical level where a possibility of ring–liner metal-to-metal contact increases. This may have pronounced effect on engine durability.

The importance of the oil film thickness measurements in an engines is not only in the numerical values of the oil film thickness but also it is fundamental to increase the knowledge about the phenomena that occurs in the piston assembly and influences the piston ring and cylinder liner contact and thus the piston ring lubrication. Among the various measurement techniques used for measuring the minimum oil film thickness in engines, the capacitance-based measurement technique has been found to deliver the most reliable results [2].

For measurement of lubricating oil film thickness between piston ring and cylinder liner, a small electrode is installed in the liner

* Corresponding author. Tel.: +91 512 259 7982; fax: +91 512 259 7408.
*E-mail address:* akag@iitk.ac.in (A.K. Agarwal).

0924-4247/$ – see front matter 
doi:10.1016/j.sna.2008.09.021

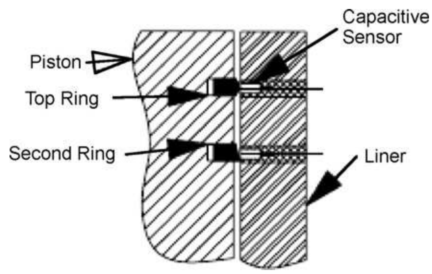


**Fig. 1.** Capacitive micro-sensors.

of the engine (Fig. 1). A parallel plate capacitor is formed between a small electrode installed in the liner and ring facing the electrode. The surface of this probe is honed flush with liner surface so that it does not cause any undesirable distinctively separate ring–liner interaction. This probe acts as a plate of capacitor. The facing area of the piston wall or ring surface in front of the probe acts as other plate of the capacitor. The separation distance between piston land and electrode varies as different parts of the piston ring assembly come in front of electrode with the reciprocating motion of the piston leading to change in capacitance thus formed. This change in capacitance is measured using an electronic circuit which converts the change in capacitance to change in voltage. This signal is recorded using a high-speed data acquisition system for data interrogation.

This method however has a limitation. The engine lubricating oil has a fixed dielectric constant and if the composition of the oil changes because of any reason (such as vapour trapping, air trapping, moisture trapping, etc. in the lubricating oil), its value will change and the sensors will over predict the oil film thickness. However since there is no other sensor, which can survive harsh environment as that of an internal combustion engine (>200 °C temp., 70–90 bar pressure, ≅10 m/s sliding speed), these errors can be ignored.

Further to these investigations, optical measurement techniques such as laser induced fluorescence technique need to be employed for more accurate measurement of oil film thickness at the ring–liner interface and the capacitance probes can be used to calibrate the LIF data under fully flooded conditions (at ring-reversal zone), where one can be reasonably sure that there is no air/vapour trapped in the lubricating oil.

## 2. Design of capacitance probe

The capacitance ($C$) of two infinite parallel conducting plates change as separation between them is varied as

$$C = K\varepsilon_0\, A/d$$

where $K$ is the dielectric constant of medium between the parallel conducting plates, $\varepsilon_0$ is the permittivity of free space, $A$ is the facing area of the two plates and $d$ is the separation distance between the two plates of the capacitor formed. Piston of the engine is grounded and hence one plate of this parallel plate capacitor is grounded. This arrangement forms two parallel plate capacitors between ground and electrode. One capacitor forms between the electrode and the piston ring and another form between back-side of the piston ring and the piston [2]. These two capacitors appear in series to give the overall capacitance $C_{\text{total}}$ which can be determined by the following equation:

$$\frac{1}{C_{\text{total}}} = \frac{1}{C_{\text{probe-ring}}} + \frac{1}{C_{\text{ring-piston}}}$$

However the plate area of the second capacitor ($C_{\text{ring-piston}}$) is very large (for present engine and sensor approximately 600 times) as compared to the first capacitor hence the second term in above equation becomes negligible, hence

$$C_{\text{total}} \approx C_{\text{probe-ring}} = \frac{K\varepsilon_0 A}{d_{\text{probe-ring}}}$$

### 2.1. Fringing of electric field

If the distance between the parallel plates is large enough then the fringing effect of electric field (converging of electric field lines at the edge of plates) can be neglected. In most of the region between the plates, the potential varies almost linearly from one plate to the other. Only near the edge of the plates, and in the regions near the outer surfaces of the plates, the electric field begins to bulge out into the universe at large so that the contours are spaced considerably further apart on the outsides of the plates than on the insides. Thus the total charge on each plate depends mostly on the field in the region between the plates. As the plates get closer and closer together, this effect becomes even more pronounced, and the charge on the outer surfaces becomes negligible compared to the charge on the inner surfaces. Furthermore, the fringing of the field at the edges of the large plates becomes a negligible part of the field structure, since it affects such a tiny part of the total plate area. The ideal formula is based on the assumptions that the charge on the outside of each plate is negligible, and that the effect of fringing can be neglected.

When plates move further apart, the contours of constant potential form ovoid around the plates; and the ovoid bulge out a bit more on the outsides of the plates than on the insides, suggesting that there is slightly more charge on the inner surface of each plate than on the outer surface. Under these conditions, the capacitance is much larger than what would be calculated from the ideal parallel plate formula.

As the distance between the plates increase even further, the ovoid become increasingly symmetrical, until they approach ellipsoids. At the limit, the plates cease to interact at all, and each plate holds a charge based only on its potential with respect to the surrounding space. Thus, as the equi-potentials approach ellipsoids, the capacitance approaches a constant value that is independent of further increases in plate distance. So from the above qualitative description of fringing effect, importance of this assumption is highlighted. It is concluded that measurement is accurate for smaller separation distances but not for larger separation distances between the ring and the liner.

Errors arising due to neglecting the fringing effect can be reduced by placing a shield around the probe electrode. This shield is put at same potential as the main electrode. Electrical insulation is maintained between the shield and the electrode. Now electric field lines start diverging after the shield hence parallel plate formula can be applied without significant error.

### 2.2. Composition of lubricating oil

For using parallel plate formula, it is assumed that region between ring and liner is fully flooded with oil, and oil is free from voids and bubbles. Presence of voids, bubbles and dissolved gases may change the value of dielectric constant. This assumption makes the magnitude of dielectric constant higher than actual value and hence over predicts the separation distance at certain locations. The actual value of $K$ also depends upon the ratio of oil and air between rings and probe, since in most situations; the ring gap is not fully flooded with oil.

### 2.3. Probe shape

Signal strength of capacitive micro-sensor depends on its face area. Large face area of central electrode causes increased capacitance input but reduced spatial resolution. The rectangular shape of probe and shield provides better spatial resolution for same probe area as compared to circular shape of sensor but the shielding is more effective in circular probes. An optimal probe would be rectangular with a large aspect ratio, having smaller length in axial direction of piston motion where high spatial resolution is required, and the length in the transverse direction chosen to maximize total plate surface area [2]. It is assumed that ring face is parallel to the probe, and the separation distance is uniform over the width and height of the probe for using parallel plate formula.

Rectangular probes with shorter length parallel to the axis of liner have been utilized in this study. This results in higher spatial resolution in the direction of ring profile. If we select a large width in transverse direction then due to circular shape of liner, the distance between two plates of capacitor (ring and central electrode) does not remain uniform, resulting in large deviation/error while using parallel plate formula. Short length in transverse direction however decreases the plate area.

The axial width of compression rings used in the engine is 2 mm; sensor width of 180 μm in axial direction ensured at least 10 data points along the face of the ring. Transverse length of 6000 μm gives a capacitance of 0.8 pF at 20 μm distance. Hence, as a compromise between spatial resolution and signal strength probe (dimension 180 μm in axial direction and 6000 μm in transverse direction) was selected as shown in Fig. 2. Probes are made of brass because it gives an optimum combination of conductivity, strength, ease of machinability and cost. Though metals like copper and silver are excellent conductor, their mechanical strength and rigidity is low. Probes of copper and silver may deform in a firing engine however probes made of brass have better dimensional integrity.

## 3. Fabrication of probe

Probes are manufactured in two parts namely outer shield and central electrode (Fig. 2). Shield is machined on milling machine, then a through hole is made by drilling and the rectangular slot for central electrode is machined using electric discharge machining (EDM) method.

Central electrode is made from thin brass shim (thickness: 0.18 mm). Its profile is achieved by cutting approximate shape and then finishing to exact dimension using diamond files. Shield increases the signal strength and minimize error in use of parallel plate formula. Shield is electrically insulated from the central electrode but kept at the same potential as that of central electrode. Hence during the assembly of the two components, thin pieces of mica sheet are pasted on electrode by using special grade high temperature epoxy.

**Fig. 2.** Assembled probe.


**Fig. 3.** Liner installed with capacitive micro-sensors.

Fiber glass insulated copper wire coaxial cable is then soldered on to the electrode and the shield for connecting them to the signal conditioning circuit.

## 4. Probe installation

Three rectangular slots (Fig. 3) were machined in the liner using EDM machine. Slots provide a clearance of 1.25 mm in transverse direction and 0.75 mm in axial direction for pasting the mica and epoxy on to the probe. Fig. 3 shows the liner with machined rectangular slots with probe installed in it.

Probe was fixed in this slot by using high temperature epoxy, which was allowed to cure for 24 h. After installing three probes at appropriate locations (Fig. 3), surface honing of the liner was carried out. There exists an outside chance of damage to extruding probes inside the liner, while honing. This was minimized by removing the excess probe material carefully using a dental grinder, and sand paper. After final honing (as done in a production grade liner), the surface profiles of the probes inside the liner were measured by a profilometer to confirm their proper installation in the liner.

## 5. Signal conditioning circuit

Measurement of the capacitance is based on the principle of impedance modulation. By this method, electrical circuit impedance presented to a calibrated (ac) sinusoidal current signal manifests, by Ohm's Law, as a corresponding ac voltage signal whose amplitude and phase are both indicative of the impedance parameters. The measurand capacitance ($C_{probe\text{-}ring}$) associated with the piston ring and the cylinder liner is incorporated in series with other resistive circuit elements to form composite impedance. This impedance is excited by a current signal derived from a voltage-to-current converter circuit being driven by a standardized voltage waveform from a sinusoidal oscillator. The oscillator is adjusted to operate at a suitably high frequency (1 MHz) consistent with the minimum response time of the measurement system. Thus as the piston undergoes displacement, the associated capacitance modulates the composite impedance yielding an output voltage

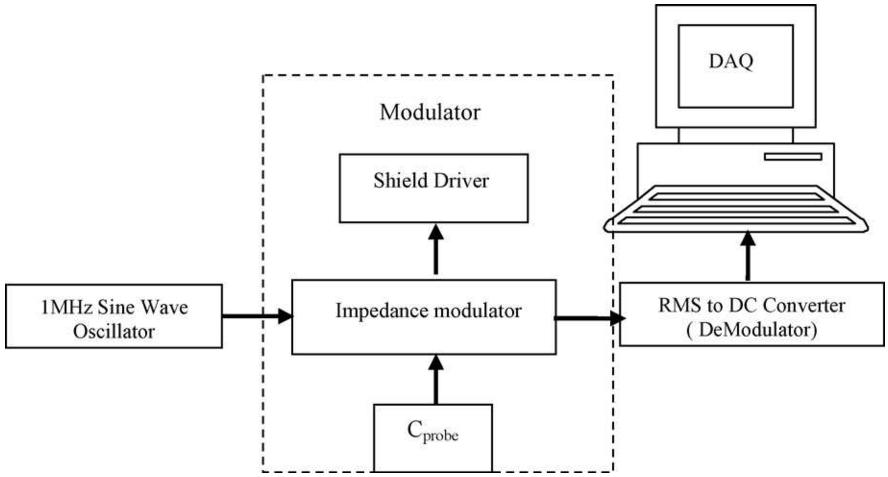


**Fig. 4.** Components of signal conditioning circuit.

signal with this modulation information present in both its amplitude and phase. This signal is next subjected to a synchronous demodulation procedure using a RMS-to-DC converter, which also receives the oscillator signal as the synchronous excitation. The emerging output from this converter is a relatively low frequency (DC) voltage, and is routed for storage into a data acquisition system so that after suitable processing, the information about the measurand capacitance can be retrieved. The shield of the probe is driven at potential of central probe through a non-inverting amplifier. Fig. 4 shows the block diagram of single channel of the signal conditioning unit.

## 6. Experimental setup

A single cylinder motored diesel engine (Make: Cooper, UK; Model: CVR-5) was used for experimental study of lubricating oil film thickness variation between the cylinder liner and piston rings. The engine was driven using an electrical motor (1 hp rated power). Speed of the motor was controlled by regulating supply voltage. The lubrication system of the motored engine was same as that of a production grade engine. Lubricating oil pump (gear pump) of the engine was used to supply the oil at a high pressure to various parts of the engine. The oil was heated externally and the temperature was maintained at 110 °C throughout the experiment.

The piston used has five rings (three compression rings, and two oil rings). The stroke length of the engine was 82 mm, liner bore diameter 82 mm, and connecting rod length is 155 mm. Top dead center (TDC) detector proximity sensor and precision shaft encoder (least count: 0.5 crank angle degree) were installed on the engine crankshaft. Voltage change due to change in capacitance and signal of the shaft encoder, TDC detector were recoded by a high-speed data acquisition system. The detailed schematic of the experimental setup is shown in Fig. 5.

## 7. Results and discussion

Sensors were calibrated by indirect calibration method, in which voltage increment corresponding to added known capacitance (low-value) was recorded and parallel plate formula correlation between capacitance and oil film thickness was used. This calibration curve is then used to convert the voltage signals to capacitance changes and then to the oil film thickness (Figs. 6–11). Data of 50 continuous cycles was recoded and viewgraphs represent average value of 50 continuous cycles. These figures represent the variation in capacitance and lubricating oil film thickness calculated for upward and downward stroke of the piston. A particular sensor observes increase in capacitance above a base value when a ring comes in front of the sensor; hence position of rings with respect to that sensor is indicated by piston profile curve in each graph. The minimum oil film thicknesses observed by sensors when they are facing rings are extremely accurate measurements. Thicknesses corresponding to interface of sensor and piston land are over predicted from actual thickness due to change in the dielectric constant of capacitor formed, because of possibility of air-entrapment in

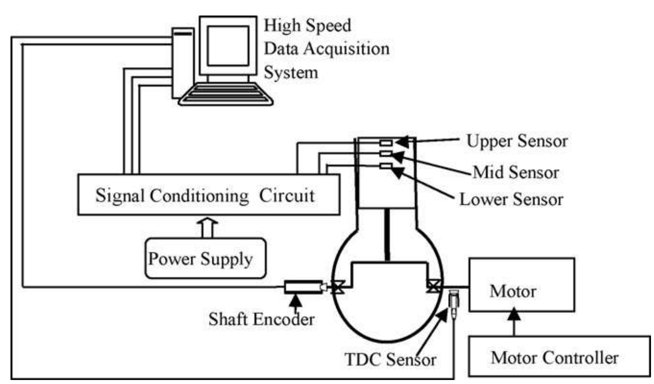


**Fig. 5.** Experimental setup.

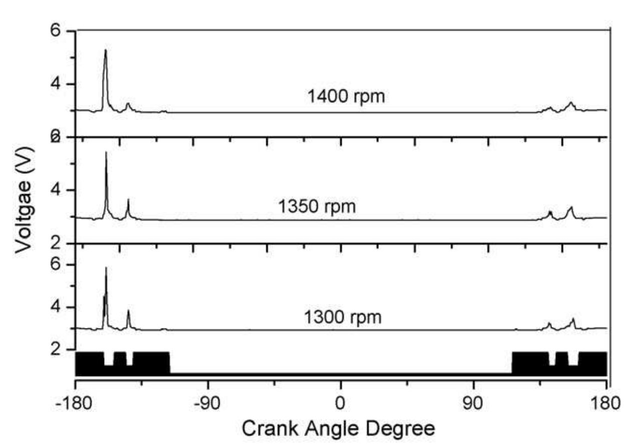


**Fig. 6.** Voltage output from upper sensor.

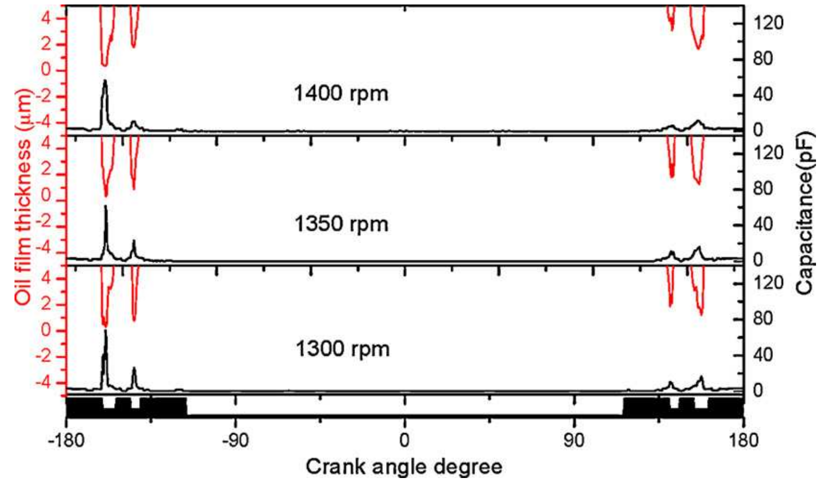


**Fig. 7.** Thickness and capacitance at upper sensor.

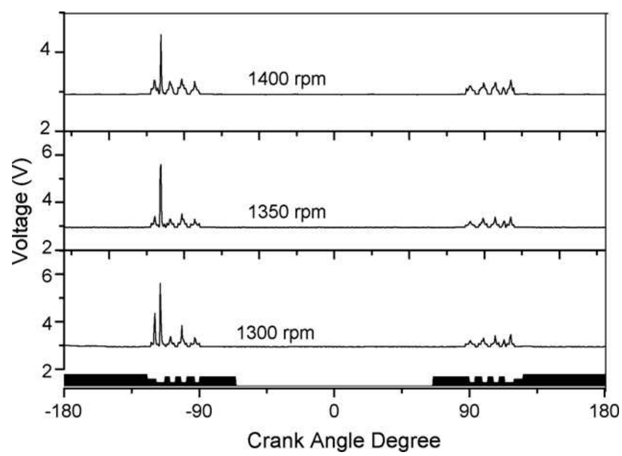


**Fig. 8.** Voltage output from middle sensor.

the oil film. At these positions, mixture of lubricating oil and air of unknown composition may be present, as against lubricating oil alone and may cause significant deviation from actual oil film thickness. Mean and percentage COV of minimum oil film thicknesses corresponding to ring–probe interface are tabulated in Tables 1–3 for the three sensor locations at different engine speeds.

**Table 1**
Minimum oil film thickness at upper sensor.

| | Downward stroke | | Upward stroke | |
|---|---|---|---|---|
| | CR1[a] | CR2[a] | CR1[a] | CR2[a] |
| CAD (1300 rpm) | −144 | −159 | 142 | 156.5 |
| MOFT (μm) | | | | |
| Mean | 0.7 | 0.2 | 1.8 | 1.2 |
| COV(%) | 2.1 | 2.0 | 2.2 | 2.6 |
| CAD (1350 rpm) | −144 | −159 | 142 | 156.5 |
| MOFT (μm) | | | | |
| Mean | 0.9 | 0.3 | 1.8 | 1.2 |
| COV(%) | 2.4 | 2.0 | 2.3 | 2.3 |
| CAD (1400 rpm) | −144 | −159 | 142 | 156.5 |
| MOFT (μm) | | | | |
| Mean | 1.8 | 0.4 | 3.1 | 1.7 |
| COV(%) | 2.4 | 2.2 | 2.1 | 2.7 |

[a] Ring.

Only top two rings cross the upper sensor as indicated by piston profile curve (Fig. 6). First groove corresponds to second compression ring and second groove corresponds to top compression ring in downward stroke (−180 to 0 CAD), and order is reversed in

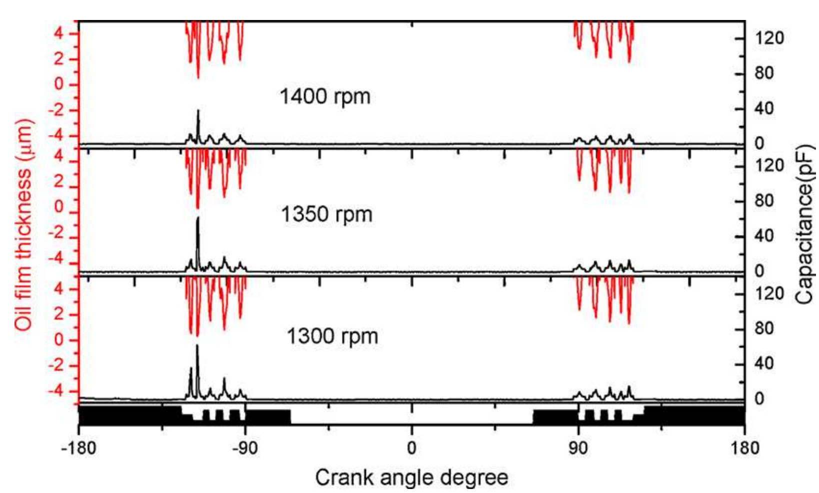


**Fig. 9.** Thickness and capacitance at middle sensor.

**Table 2**
Minimum oil film thickness corresponding to rings at middle sensor.

| | Downward stroke | | | | | Upward Stroke | | | | |
|---|---|---|---|---|---|---|---|---|---|---|
| | CR1[a] | CR2[a] | CR3[a] | OR1[a] | | CR1[a] | CR2[a] | CR3[a] | OR1[a] | |
| CAD (1300 rpm) | −93 | −101.5 | −109.5 | −115.5 | −120 | 90.5 | 99.5 | 107.5 | 112.5 | 117.5 |
| MOFT (μm) | | | | | | | | | | |
| Mean | 1.7 | 0.8 | 1.5 | 0.3 | 0.6 | 2.4 | 2.8 | 1.4 | 2.1 | 1.3 |
| COV(%) | 2.3 | 2.1 | 2.3 | 3.1 | 3.4 | 2.1 | 2.2 | 2.6 | 3.3 | 3.2 |
| CAD (1350 rpm) | −93 | −101.5 | −109.5 | −115.5 | −120 | 90.5 | 99.5 | 107.5 | 112.5 | 117.5 |
| MOFT (μm) | | | | | | | | | | |
| Mean | 1.8 | 1.2 | 1.9 | 0.3 | 1.4 | 2.5 | 1.9 | 1.5 | 2.3 | 1.5 |
| COV(%) | 2.3 | 2.4 | 2.2 | 3.3 | 3.5 | 2.6 | 2.2 | 2.5 | 3.4 | 3.6 |
| CAD (1400 rpm) | −93 | −101.5 | −109.5 | −115.5 | −120 | 90.5 | 99.5 | 107.5 | 112.5 | 117.5 |
| MOFT (μm) | | | | | | | | | | |
| Mean | 1.9 | 1.6 | 1.9 | 0.5 | 1.8 | 2.8 | 2.1 | 2.1 | 3.4 | 1.8 |
| COV(%) | 2.1 | 2.4 | 2.3 | 3.4 | 3.6 | 2.2 | 2.5 | 2.3 | 3.6 | 3.3 |

[a] Ring.

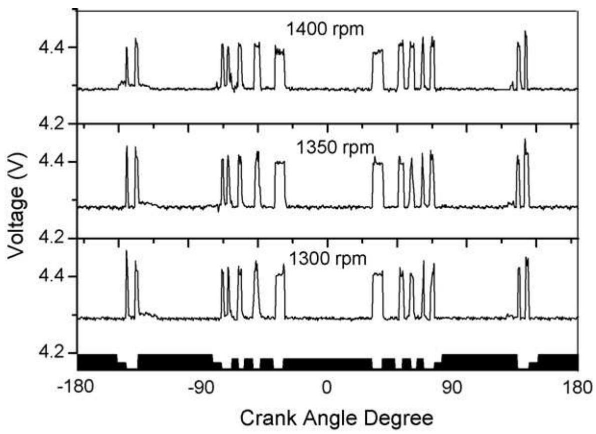


**Fig. 10.** Voltage output from lower sensor.

upward stroke (0–180 CAD). Second pressure ring comes in front of upper sensor from −159 to −153 CAD in downward stroke and from 153 to 159 CAD in upward stroke. First compression ring comes in front of sensor from −145 to −141 CAD in downward stroke and from 141 to 145 CAD in upward stroke. On comparing the minimum oil film thickness position to sensor contact duration in first compression ring (Fig. 7), it comes to about middle of the groove suggesting barrel shape of the first compression ring. The inclined shape of second ring is also visible in thickness profile of the second compression ring, suggesting its axial movement along the width.

Top four rings cross the middle sensor (Figs. 8 and 9). First groove corresponds to first oil ring, and other three grooves on piston profile curve indicate the compression rings in the order in the downward stroke of the piston. First oil ring comes in front of sensor from −120 to −114.5 CAD in downward stroke and from 114.5 to 120 in upward stroke. Third compression ring comes in front of middle sensor from −109.5 to −107 CAD in downward stroke and from 107 to 109.5 CAD in upward stroke of the engine. Second compression ring faces the middle sensor from −102.5 to −99.5 CAD in downward stroke and from 89.5 to 92 in upward stroke of the engine. First compression ring faces the sensor from −93 to −91 CAD in downward stroke and from 91 to 93 in upward stroke of the engine. Middle sensor remains uncovered from −65.5 to 65.5 CAD. All the rings come in front of sensor when the piston linear speed is relatively high, being located in the middle of the stroke.

Minimum lubricating oil film thickness for various rings at middle sensor is shown in Table 2 at engine speeds of 1300, 1350 and 1400 rpm, respectively. Minimum oil film thickness in upward

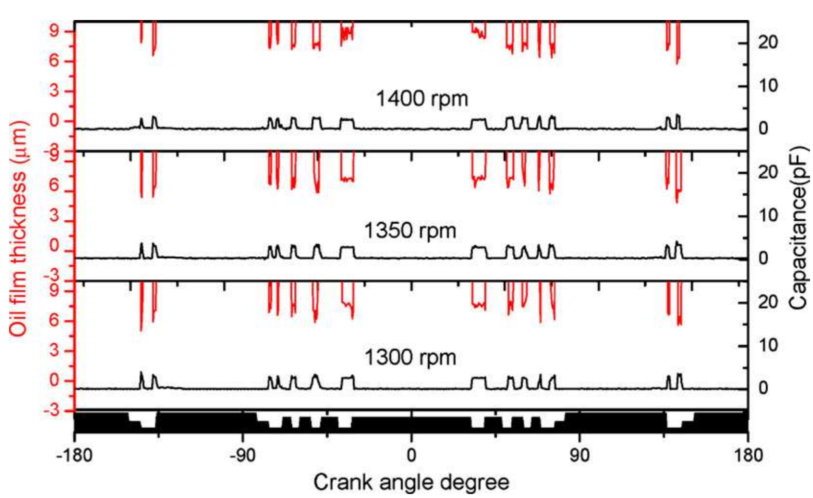


**Fig. 11.** Thickness and capacitance at lower sensor.

**Table 3**
Minimum oil film thickness corresponding to various rings at lower sensor.

| | Downward stroke | | | | | | | Upward stroke | | | | | | |
|---|---|---|---|---|---|---|---|---|---|---|---|---|---|---|
| | CR1[a] | CR2[a] | CR3[a] | OR1[a] | | OR2[a] | | CR1[a] | CR2[a] | CR3[a] | OR1[a] | | OR2[a] | |
| CAD (1300 rpm) | −31.5 | −51.5 | −64 | −71.5 | −78 | −138 | −144.5 | 39.5 | 48.5 | 63 | 72.5 | 76.5 | 135 | 144 |
| MOFT (μm) | | | | | | | | | | | | | | |
| Mean | 6.3 | 5.9 | 6.4 | 6.6 | 6.8 | 5.9 | 5 | 7.1 | 6.6 | 7.4 | 5.9 | 6.2 | 6.6 | 5.5 |
| COV(%) | 2.1 | 2.4 | 2.2 | 3.2 | 2.9 | 3.9 | 3.7 | 2.3 | 2.2 | 2.2 | 2.7 | 2.6 | 3.8 | 3.9 |
| CAD (1350 rpm) | −31.5 | −51.5 | −64 | −71.5 | −78 | −138 | −144.5 | 39.5 | 48.5 | 63 | 72.5 | 76.5 | 135 | 144 |
| MOFT (μm) | | | | | | | | | | | | | | |
| Mean | 7 | 7 | 6.4 | 7.2 | 6.8 | 5.9 | 5.4 | 7.1 | 6.5 | 6.5 | 6 | 6.2 | 6.7 | 5.9 |
| COV(%) | 2.2 | 2.4 | 2.3 | 2.8 | 2.7 | 3.8 | 3.6 | 2.0 | 2.2 | 2.1 | 2.8 | 2.9 | 3.8 | 3.7 |
| CAD (1400 rpm) | −31.5 | −51.5 | −64 | −71.5 | −78 | −138 | −144.5 | 39.5 | 48.5 | 63 | 72.5 | 76.5 | 135 | 144 |
| MOFT (μm) | | | | | | | | | | | | | | |
| Mean | 8.2 | 7.6 | 7.2 | 7.6 | 7.4 | 6.6 | 7.9 | 8.3 | 6.7 | 7 | 6.4 | 7.4 | 7.2 | 6.3 |
| COV(%) | 2.2 | 2.1 | 2.0 | 2.7 | 3.0 | 3.5 | 3.7 | 2.4 | 2.3 | 2.4 | 2.6 | 3.1 | 3.6 | 3.7 |

[a] Ring.

stroke is higher than oil film thickness in downward stroke due to piston tilt towards sensor side of the liner at upper edge in downward stroke and tilting of lower edge of piston towards sensor in upward stroke. Since all the rings facing the middle sensor lie above gudgeon pin hence this tilting decreases the film thickness in downward stroke as compared to upward stroke.

All five rings pass in front of the lower sensor (Figs. 10 and 11). First grove corresponds to second oil ring, second groove corresponds to first oil ring and the next three grooves represent the compression rings in downward stroke of the piston, and this order is reversed in the upward stroke.

Second oil ring comes in front of lower sensor from −143 to −137 CAD in downward stroke and from 137 to 143 CAD in upward stroke. First oil ring faces the lower sensor from −76.5 to −71 CAD in downward stroke and 71–76.5 CAD in upward stroke. Third compression ring comes in front of lower sensor from −64 to −60.5 CAD in downward stroke and 60.5–64 CAD in upward stroke of the engine. Second compression ring faces the lower sensor from −52 to −48 CAD in downward stroke and from 48 to 52 CAD in upward stroke of the engine. First compression ring comes in front of lower senor from −37.5 to −33.5 in downward stoke and from 33.5 to 37.5 in upward stroke of the engine.

Fig. 12 shows the MOFT for first compression ring at TDC, Mid stroke and BDC position in downward and upward stroke of the engine. Minimum oil film thicknesses are compared at different speeds at a location. MOFT generally increases with speed at every position. MOFT at mid stroke is more as compared to TDC because at mid stroke, piston speed is high as compared to TDC, which results in less squeezing effect at mid stroke, where hydrodynamic lubrication conditions dominate. MOFT at BDC is quite large as compared to TDC.

Fig. 13 shows the MOFT for second compression ring at TDC, Mid stroke and BDC position in downward and upward strokes. MOFT in upward stroke of the engine are more than film thickness in downward stoke due to tilting of piston towards the sensor in downward stroke and away from the sensor in upward stroke for second compression ring. Generally minimum oil film thickness increases with engine speed.

Fig. 14 shows MOFT for third compression ring at mid stroke and BDC in upward and downward stroke at various speeds. There is no

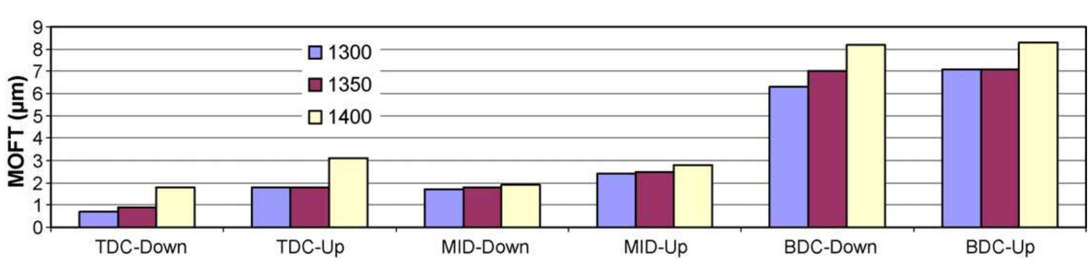


**Fig. 12.** Minimum oil film thickness for first compression ring.

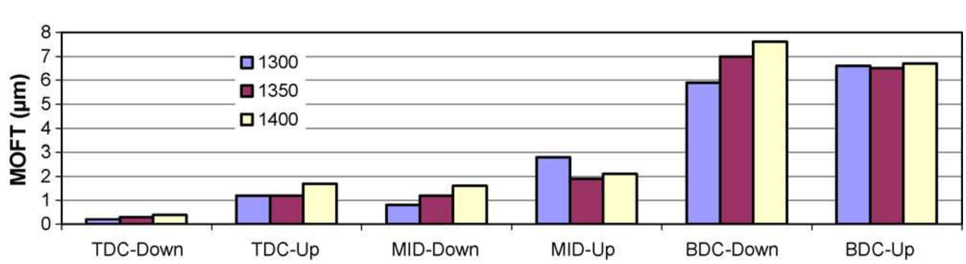


**Fig. 13.** Minimum oil film thickness for second compression ring.

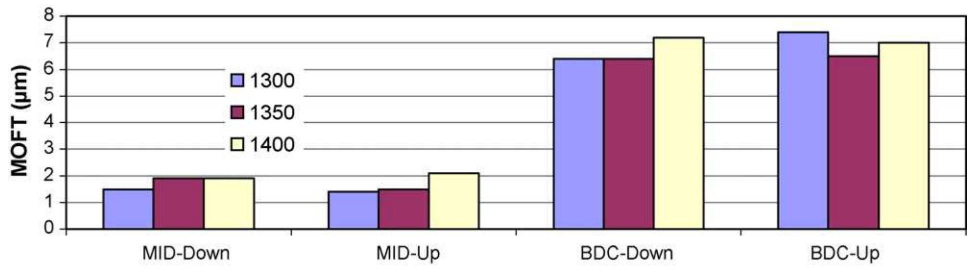


**Fig. 14.** Minimum oil film thickness for third compression ring.

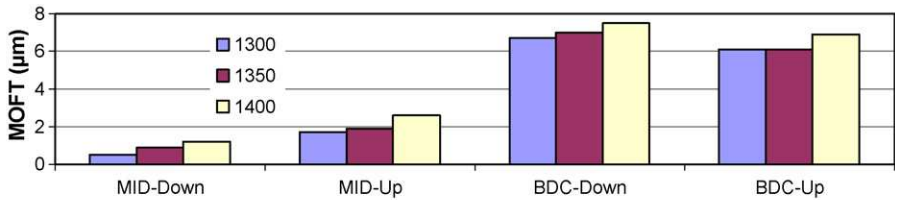


**Fig. 15.** Minimum oil film thickness for first oil ring.

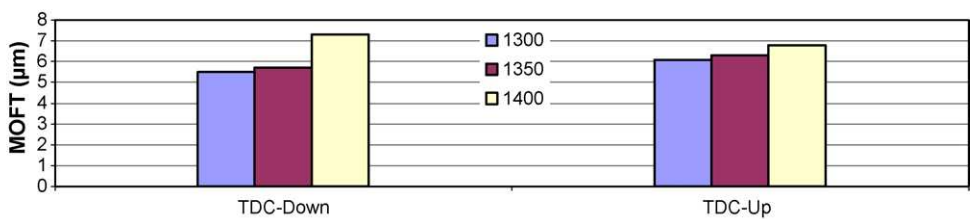


**Fig. 16.** Minimum oil film thickness for second oil ring.

significant difference in MOFT in upward and downward stroke at mid stroke because piston tilt does not cause significant change in piston liner separation at the middle of the piston.

Fig. 15 shows minimum lubricating oil film thickness for first oil ring at mid stroke and BDC in upward and downward stroke of engine at various speeds. MOFT at BDC is comparatively large because liner bore diameter at that position is large. It is also observed that MOFT generally increases with increasing engine speed for first oil ring.

Fig. 16 shows minimum lubricating oil film thickness for second oil ring at TDC in upward and downward stroke of engine at various speeds. Second oil ring comes in front of lower sensor at −144.5 to −136.5 CAD in downward stroke and 136.5–144.5 CAD in upward stroke, when piston reaches near TDC. Oil film thickness was found to increases with piston speed.

## 8. Conclusions

The capacitance probes and associated electronic circuit is developed for measurement of minimum oil film thickness in a motored engine. Measurement of capacitance formed between the piston ring and a probe mounted flush in the liner provided an accurate measurement of the oil film thickness, based on the assumption that the region between the probe and liner was fully flooded with lubricating oil whose dielectric constant is known. Various experiments for measurement of lubricating oil film thickness were conducted at different engine speeds and the parameters were measured at three different locations in the liner. Lubricating oil film thickness was found to vary between 0.2 and 8 μm in the motored engine. At any particular position, lubricating oil film thickness varies significantly in upward and downward stroke of the engine due to reversal in direction of piston tilt in the two strokes. This variation was comparatively small as compared to fired engine data reported by other researchers [2–8] due to absence of gas compression and combustion pressure in the engine simulator. Lubricating oil film thickness was found to increase with increasing engine speed at all positions of sensors. This is because of shift of lubrication regime from boundary/mixed lubrication to hydrodynamic regime.

## Acknowledgements

The authors acknowledge financial grant from *Ministry of Human Resource Development, Government of India* for pursuing this research. The grant was provided for the project entitled "Development of Capacitance Based Micro-Sensor for Oil Film Thickness Measurements", to be carried out at IIT Kanpur (2004–2006).

## References

[1] J.B. Heywood, Fundamentals of Internal Combustion Engine, Mc-Graw Hill, 1988.
[2] R.J. Donahue, D.O. Ducu, J.B. Ghandhi, Design of capacitance probes for oil film thickness measurements between the piston ring and liner in internal combustion engines, Journal of Engineering for Gas Turbines and Power 123 (2001) 633–643.
[3] L. Shenghua, L. Jijun, Z. Lonbao, W. Rong, An Experimental Investigation of the Oil Film Lubricating Piston Rings, SAE Paper No. 961912, 1996.
[4] T. Seki, K. Nakayama, T. Yamada, A. Yoshid, M. Takiguchi, A study on variation in oil film thickness of a piston ring package: variation of oil film thickness in piston sliding direction, JSAE Review 21 (3) (2000) 315–320.
[5] C. Mattsson, Measurement of the Oil Film Thickness between the Cylinder Liner and the Piston Rings in a Heavy Duty Direct Injection Diesel Engine, SAE Paper No. 952469, 1995.
[6] M. Takiguchi, K. Nakayama, S. Furuhama, H. Yoshida, Variation of Piston Ring Oil film Thickness in an Internal Combustion Engine, SAE Paper No 980563, 1998.

[7] M. Takiguchi, R. Sasaki, I. Takahashi, F. Ishibashi, S. Furuhama, R. Kai, M. Sato, Oil Film Thickness Measurement and Analysis of a Three Ring Pack in an Operating Diesel Engine, SAE Paper No.2000-01-1787, 2000.
[8] J.B. Ghandhi, Single and dual-fiber fluorescence probes: application to oil-film measurements in an internal combustion engine, Applied Optics 39 (30/20) (2000) 5456–5464.
[9] I. Sherrington, E.H. Smith, Experimental methods for measuring the oil-film thickness between the piston-rings and cylinder-wall of internal combustion engines, Tribology International 18 (6) (1985) 315–320.
[10] B. Thirouard, T. Tian, D.P. Hart, Investigation of Oil Transportation Mechanisms in the Piston Ring Pack of a Single Cylinder Diesel Engine, Using Two Dimensional Laser Induced Fluorescence, SAE Paper No. 982658, 1998.
[11] T. Tian, V.W. Wong, J.B. Heywood, Modeling the Dynamics and Lubrication of Three Piece Oil Control Rings in Internal Combustion Engines, SAE Paper No. 982657, 1998.
[12] C. Arcoumanis, M. Duszynski, H. Flora, P. Ostovar, Development of a Piston Ring Lubrication Test-rig and Investigation of Boundary Conditions for Modeling Lubricant Film Properties, SAE Paper No. 952468, 1995.

## Biographies

**Atul Dhar** is a Graduate student working with Dr. Agarwal on his doctoral dissertation in mechanical engineering from IIT Kanpur. He is a graduate of mechanical engineering from HBTI, Kanpur (2004) and he completed his Master's in Thermal Engineering from IIT Kanpur in the year 2006. His areas of interest include Internal Combustion Engines, micro-sensor development, emission control and combustion.

**Dr. Avinash Kumar Agarwal** is currently working as Associate Professor of Mechanical Engineering at Indian Institute of Technology, Kanpur since March 2001. He is a 1994 Mechanical Engineering graduate from MREC Jaipur. His area of doctoral research at Indian Institute of Technology Delhi was developing biodiesel and related engine tribology investigations. Dr. Agarwal joined Engine Research Center, University of Wisconsin, Madison, USA for pursuing his Post-Doctoral research from August 1999 to February 2001. His main areas of current interest are combustion phenomenon study in IC engines, automobile emissions, biodiesel development and characterization, laser diagnostic techniques, PIV, lubricating oil consumption phenomenon, lubricating oil tribology, development of micro-sensors, alternative fuels for diesel engines, etc.

**Mr. Vishal Saxena** is a Principal Research Engineer at Department of Electrical Engineering at Indian Institute of Technology Kanpur. He graduated in electrical engineering from IIT Kanpur in 1973. He completed his M.Tech. from the same department in 1990. His research areas include instrumentation, micro-processor and control.